**Supplementary Material**

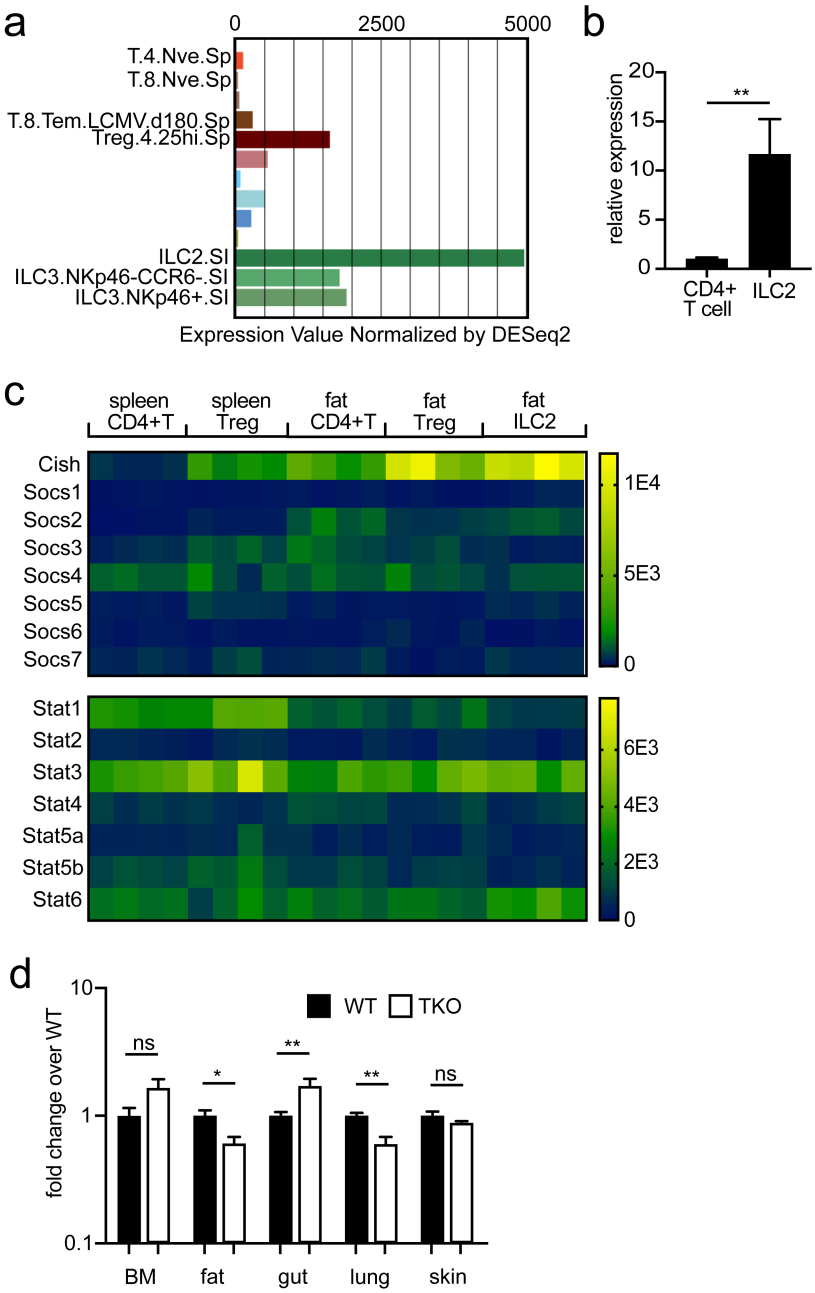


Supplementary Figure 1: CISH is highly expressed in tissue ILC2s. **a** *Cish* is highly expressed in ILC2s compared to other leukocytes. Data adapted from ImmGen. **b** Expression of *Cish* in lung ILC2s or CD4+ T cells. **p<0.01 by 2-tailed t-test. n = 4 mice/tissue. **c** RNA sequencing from purified ILC2s from multiple tissues ILC2s as compared to other tissue resident lymphocytes.

Legend colors indicate counts per million reads. **d** *Cish* expression in WT or Il25$^{-/-}$/Crlf2$^{-/-}$/Il1rl1$^{-/-}$ ("TKO") mice. *p<0.05, **p<0.01, ns=non-significant by unpaired t-test. n = 3-7 mice/group.

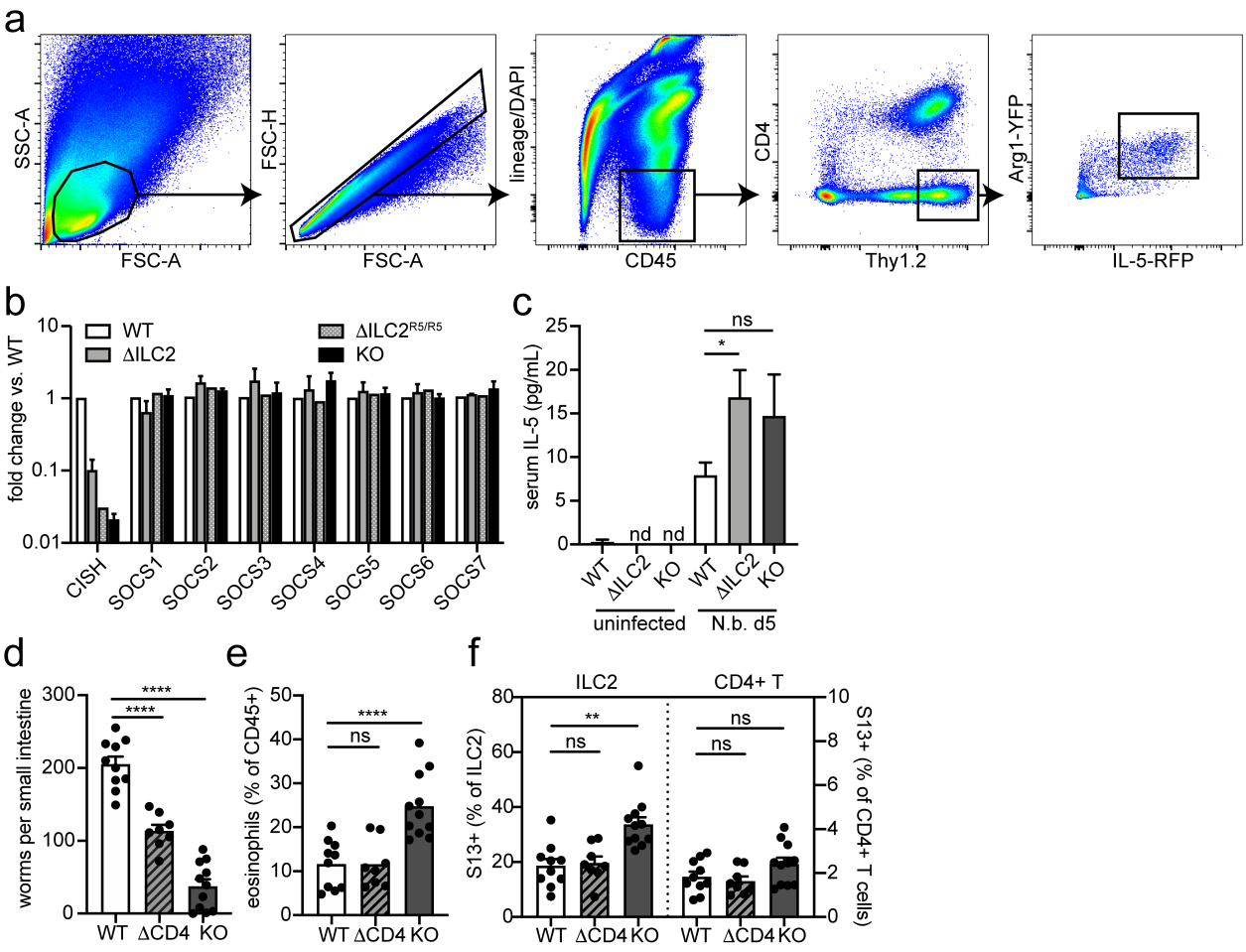


Supplementary Figure 2: CISH knockdown in ILC2s or T cells leads to augmented immunity to helminth challenge. **a** Representative gating strategy for lung ILC2s. **b** Expression of *Cish* and other SOCS family members in lung ILC2s measured by qPCR. ΔILC2$^{R5/R5}$ indicates homozygous expression of R5. Statistics shown for *Cish* in Figure 1a; all others non-significant. n = 3 mice/group. **c** Serum IL-5 measured at day 5 of infection with *N.b.* as in Figure 2. *p<0.05. n = 6 mice/group. **d** Number of *N.b.* worms in SI on day 5. ****p<0.0001 for one-way ANOVA with Dunnett testing for multiple comparisons. n = 8-11 mice/group; data pooled from 2 similar experiments. **e** Lung eosinophils on infection day 5. ***p<0.001; ns = non-significant for one-way ANOVA with Dunnett testing for multiple comparisons. n = 8-11 mice/group; data pooled from 2 similar experiments. **f** IL-13 expression (S13) on ILC2s or CD4+ T cells at day 5 of infection.

**p<0.01 for Brown-Forsythe and Welch ANOVA with Dunnett correction for multiple comparison. ns=non-significant. n = 8-11 mice/group pooled from 2 similar experiments.

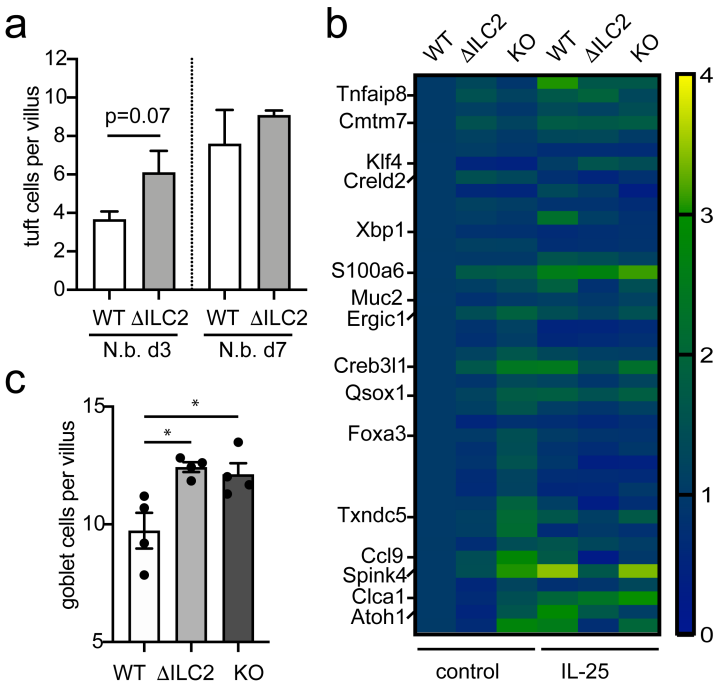


Supplementary Figure 3: CISH constraint of ILC2 outputs controls secretory cell development in the intestine. **a** Tuft cells per villus counted from immunofluorescence staining of intestines from *N.b.*-infected mice at indicated timepoints. Numbers indicate average +/- SEM over a minimum of 10 intact villi from each of 4-5 mice/group. **b** Goblet cell markers in whole intestinal tissue harvested from IL-25- or untreated mice. Each block represents row-normalized mean expression in 3 mice/group. **c** Goblet cells counted from PAB-stained sections of untreated mice of indicated genotypes. Numbers indicate average +/- SEM over a minimum of 10 intact villi from each of 4 mice/group. *P<0.05 by one-way ANOVA with Dunnett testing for multiple comparisons.

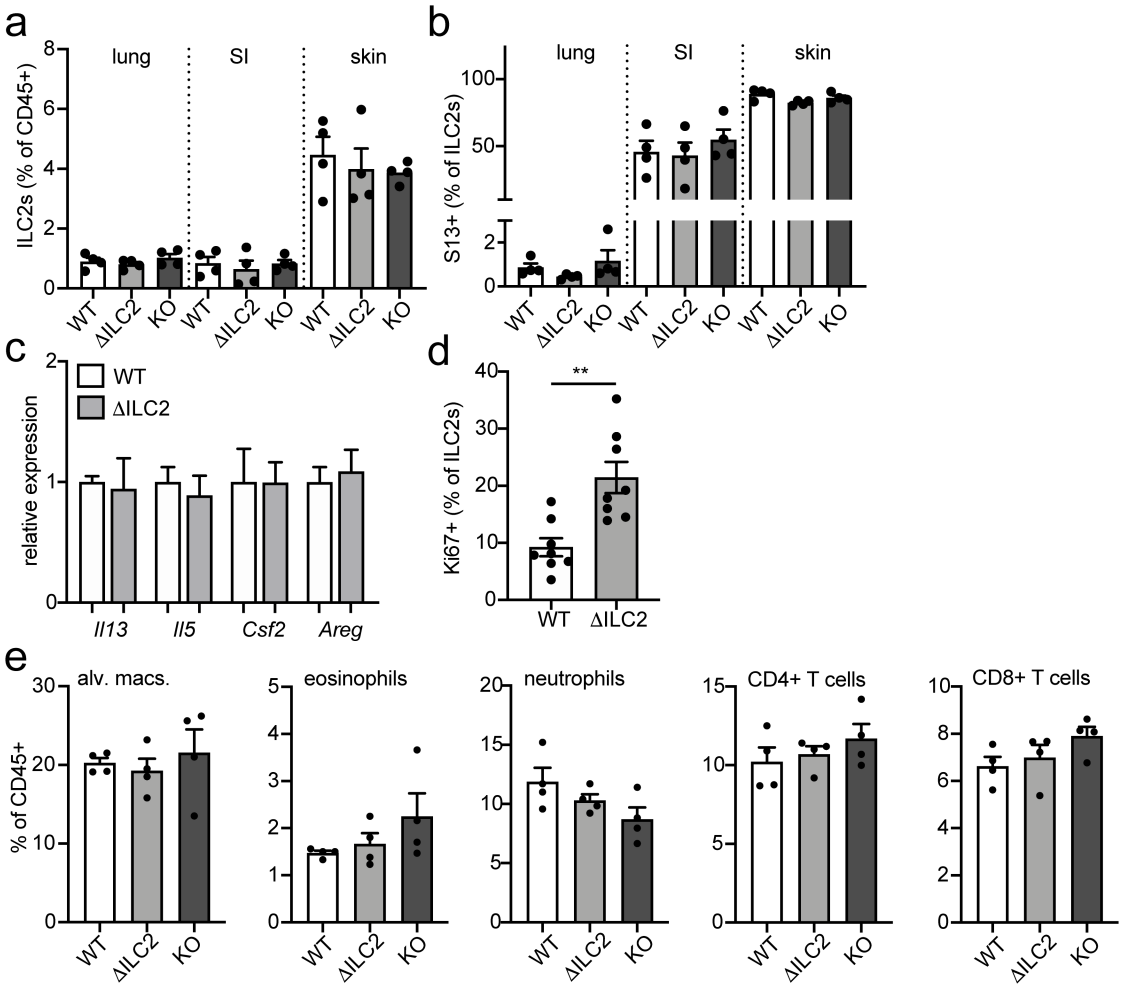


Supplementary Figure 4: Loss of CISH in ILC2s yields increased tissue ILC2 turnover without affecting steady state numbers. **a** Proportion of ILC2s in the lung, SI, and skin. n = 4 mice/group, representative of 2 similar experiments. **b** IL-13 expression in ILC2s in the lung, SI, and skin. n = 4 mice/group. **c** Expression of indicated effector genes in sorted lung ILC2s. n = 3-9 mice/group, pooled from 2 of 3 similar experiments. **d** Ki67 expression measured by flow cytometry from freshly-isolated SI ILC2s. n = 8 mice/group, pooled from 2 similar experiments. **p<0.01. **e** Leukocyte subsets (as indicated) in from lung of untreated mice. n = 4 mice/group, representative of 2 similar experiments.

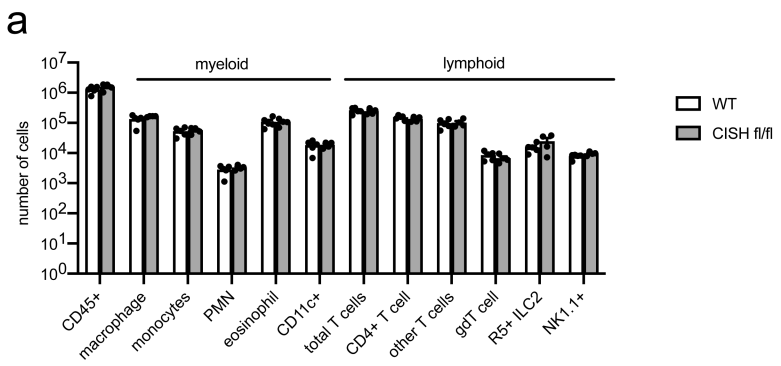


Supplementary Figure 5: Loss of CISH in ILC2s yields no significant differences in numbers of intestinal immune cells during *Salmonella* infection. **a** number of cells counted per centimeter of jejunum.

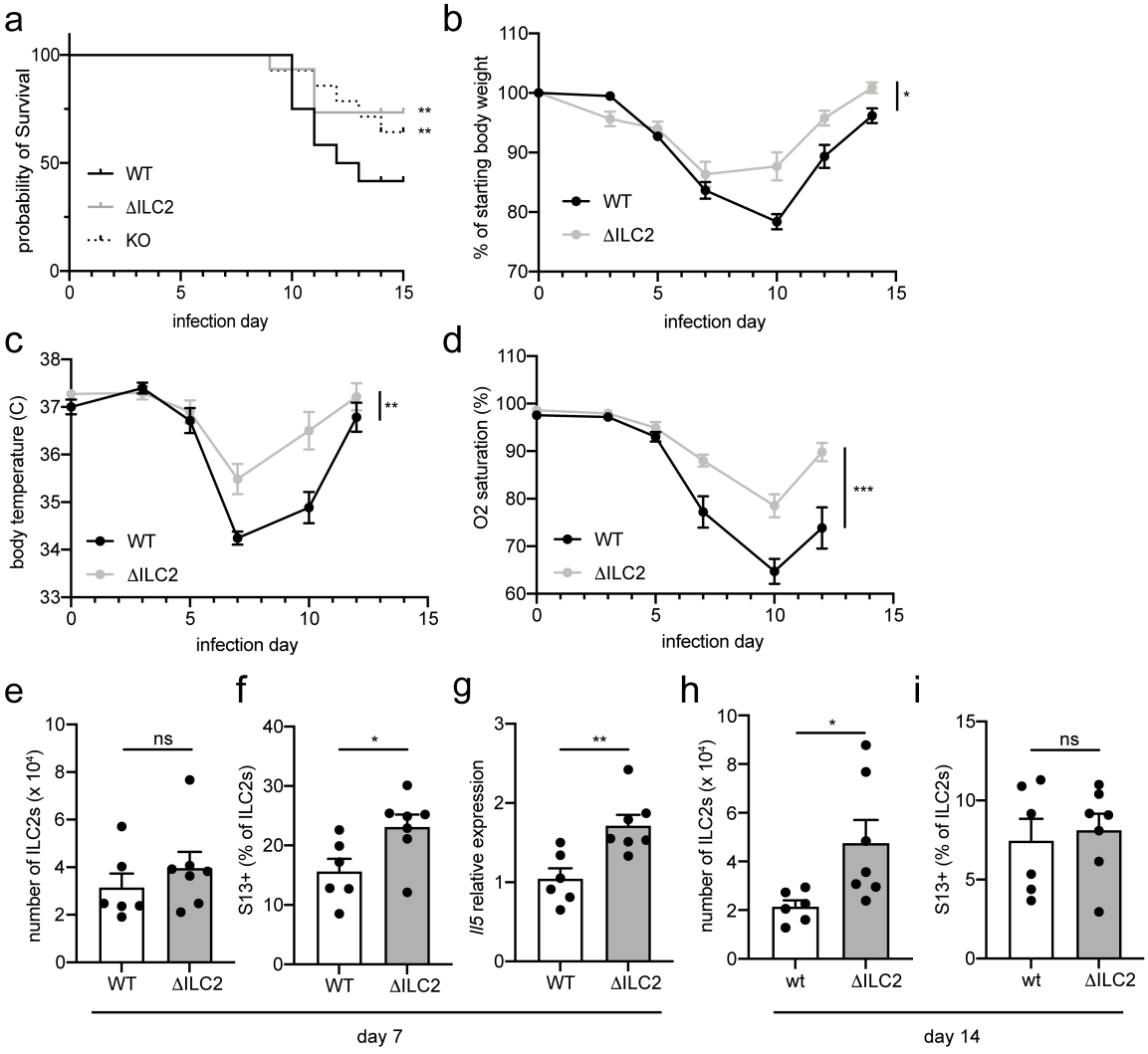


Supplementary Figure 6: Augmented ILC2 activity through CISH deletion improves survival during influenza infection. **a** Survival after influenza PR8 in indicated strains. n = 12-15 mice per group, pooled from two experiments. **b** Body weight, **c** body temperature and, **d** oxygen saturation measured in indicated genotypes. for (a-d), *p<0.05, **p<0.01, ***p<0.001 for differences between genotype by 2-way ANOVA. n = 7 mice/group. **e** Number of lung ILC2s and **f** S13 reporter expression on lung ILC2s on day 7 of influenza infection. **g** *Il5* transcripts in whole lung tissue on day 7 of influenza infection. **h** number of lung ILC2s and **i** S13 reporter

expression on lung ILC2s on day 14 of influenza infection. for (e-i), *p<0.05, **p<0.01, ns = non-significant by t-test. n = 6-7 mice/group.

Supplementary Table 1: Antibodies used

Supplementary Table 2: Primers used for qRT-PCR

| Gene symbol | Forward Primer | Reverse Primer |
|---|---|---|
| *Areg* | CAGCTATTGGCATCGGCATC | TTCAACTTTTACCCTGCATTGTCC |
| *Ccl2* | AGGTCCCTGTCATGCTTCTGG | CTGCTGCTGGTGATCCTCTTG |
| *Cd36* | GCTTGCAACTGTCAGCACAT | GCCTTGCTGTAGCCAAGAAC |
| *Chil3* | CAGGTCTGGCAATTCTTCTGAA | GTCTTGCTCATGTGTGTAAGTGA |
| *Cish* | ATGGTCCTTTGCGTACAGGG | GGAATGCCCCAGTGGGTAAG |
| *Clec10a* | CAGAATCGCTTAGCCAATGTGG | TCCCAGTCCGTGTCCGAAC |
| *Csf2* | TCAGAGAGAAAGGCTAAGGTCC | CTCTTCATTCAACGTGACAGGC |
| *Cxcl10* | CCAAGTGCTGCCGTCATTTTC | GGCTCGCAGGGATGATTTCAA |
| *Cxcl9* | TCCTTTTGGGCATCATCTTCC | TTTGTAGTGGATCGTGCCTCG |
| *Hprt* | GTTGGATACAGGCCAGACTTTGTTG | GAGGGTAGGCTGGCCTATAGGCT |
| *Ifng* | CATTGAAAGCCTAGAAAGTCTGAATAAC | TGGCTCTGCAGGATTTTCATG |
| *Il10* | GCTGGACAACATACTGCTAACCG | CCTTGCTCTTATTTTCACAGGGG |
| *Il13* | GGATATTGCATGGCCTCTGTAAC | AACAGTTGCTTTGTGTAGCTGA |
| *Il17a* | AGCAGCGATCATCCCTCAAAG | GTCTTCATTGCGGTGGAGAGTC |
| *Il2* | TGAGCAGGATGGAGAATTACAGG | GTCCAAGTTCATCTTCTAGGCAC |
| *Il22* | TCAGACAGGTTCCAGCCCTA | CAGGTCCAGTTCCCCAATCG |
| *Il4* | GCTCGTCTGTAGGGCTTCC | GTGCAGCTTATCGATGAATCCAG |
| *Il5* | CTCTGTTGACAAGCAATGAGACG | TCTTCAGTATGTCTAGCCCCTG |
| *Il9* | ATGTTGGTGACATACATCCTTGC | TGACGGTGGATCATCCTTCAG |
| *Nos2* | GAATCTTGGAGCGAGTTGTGG | CAGGAAGTAGGTGAGGGCTTG |
| *Retnla* | CCAATCCAGCTAACTATCCCTCC | ACCCAGTAGCAGTCATCCCA |
| *Rpl13a* | GAGGTCGGGTGGAAGTACCA | TGCATCTTGGCCTTTTCCTT |
| *Tnfa* | TCTGTCTACTGAACTTCGGGGTG | ACTTGGTGGTTTGCTACGACG |

Supplementary Table 3: List of gene symbols for consensus “tuft cell” and “goblet cell” identities corresponding to heatmaps in Figure 3c and Supplementary Figure 3b

Supplementary Table 4: Selected outputs from Gene Set Enrichment Analysis

Supplementary Table 1: Antibodies used

| Antigen | Clone | vendor | Catalog # |
|---|---|---|---|
| **Anti-Mouse FACS antibodies** | | | |
| Anti-mouse CD45 BUV395 | 30-F11 | BD | Cat# 565967 |
| Anti-mouse CD45 BV 711 | 30-F11 | BioLegend | Cat# 103147 |
| Anti-mouse CD125 PE | T21 | BD Biosciences | Cat# 558488 |
| Anti-mouse SiglecF PerCP-Cy™5.5 | E50-2440 | BD Biosciences | Cat# 565526 |
| Anti-mouse CD11b BV650 | M1/70 | BioLegend | Cat# 101239 |
| Anti-mouse CD11c BV785 | N418 | BioLegend | Cat# 117335 |
| Anti-mouse CD127 APC-eFluor® 780 | A7R34 | eBioscience/ThermoFisher | Cat# 47-1271-82 |
| Anti-mouse Gr-1 APC | RB6-8C5 | BioLegend | Cat# 108412 |
| Anti-mouse ST2 PE | DJ8 | MD Biosciences | Cat# 101001PE |
| Anti-mouse ST2 Biotin | DJ8 | MD Biosciences | Cat# 101001B |
| Anti-mouse CD3 PE-Cy7 | 17A2 | BioLegend | Cat# 100220 |
| Anti-mouse CD3 APC-Cy7 | 17A2 | BioLegend | Cat# 100222 |
| Anti-mouse CD3 BV711 | 17A2 | BioLegend | Cat# 100241 |
| Anti-mouse Thy1.2 BV605 | 53-2.1 | BioLegend | Cat# 140317 |
| Anti-mouse Thy1.2 BV785 | 30-H12 | BioLegend | Cat# 105331 |
| Anti-mouse CD4 PerCP | RM4-5 | eBioscience/ThermoFisher | Cat# 45-0042-82 |
| Anti-human/mouse GATA3 AF488 | TWAJ | eBioscience/ThermoFisher | Cat# 53-9966-42 |
| Anti-mouse Foxp3 PE | FJK-16s | eBioscience/ThermoFisher | Cat# 12-5773-82 |
| Anti-mouse T-bet PE-Cy7 | 4B10 | eBioscience/ThermoFisher | Cat# 25-5825-80 |
| Anti-mouse Ki67 FITC | SolA15 | eBioscience/ThermoFisher | Cat# 11-5698-82 |
| **Anti-Mouse Lineage cocktail** | | | |
| Anti-mouse CD8a PB | 53-6.7 | BioLegend | Cat# 100725 |
| Anti-mouse CD49b PB | DX5 | BioLegend | Cat# 108918 |
| Anti-mouse NK-1.1 PB | PK136 | BioLegend | Cat# 108722 |
| Anti-mouse Gr-1 PB | RB6-8C5 | BioLegend | Cat# 108430 |
| Anti-mouse TER-119 PB | TER-119 | BioLegend | Cat# 116232 |
| Anti-mouse FcεRIa PB | Mar-1 | BioLegend | Cat# 134314 |
| Anti-mouse CD3 PB | 17A2 | BioLegend | Cat# 100214 |
| Anti-mouse CD19 PB | 6D5 | BioLegend | Cat# 115523 |
| Anti-mouse CD11c PB | N418 | BioLegend | Cat# 117322 |
| Anti-mouse/human CD11b PB | M1/70 | BioLegend | Cat# 101224 |

| | | | |
|---|---|---|---|
| Anti-mouse CD4 PB | RM4-5 | BioLegend | Cat# 100534 |
| Anti-mouse F4/80 PB | BM8 | BioLegend | Cat# 123124 |
| **Anti-human FACS antibodies** | | | |
| Anti-human CD4 APC | RPA-T4 | eBioscience | Cat# 17-0049 |
| **Immunofluorescence** | | | |
| Anti-mouse DCLK1 | polyclonal | Abcam | Cat# ab31704 |
| Anti-RFP | polyclonal | SicGen | Cat# AB8181 |
| Anti-mouse EpCAM AF647 | G8.8 | BioLegend | Cat# 118211 |
| Goat anti-rabbit IgG AF488 | polyclonal | Invitrogen | Cat# A-11070 |
| Donkey anti-goat IgG AF555 | polyclonal | Invitrogen | Cat# A-21432 |

Supplementary Table 3: Gene symbols for consensus “tuft” and “goblet” identities corresponding to heatmaps in Fig. 3c and Suppl. Fig. 3b

| **Tuft cell** | |
|---|---|
| *Dclk1* | *Tmem176a* |
| *Alox5ap* | *Smpx* |
| *Sox9* | *Itpr2* |
| *Spib* | *Siglecf* |
| *Avil* | *Ffar3* |
| *Trpm5* | *Rac2* |
| *Il17rb* | *Hmx2* |
| *Chat* | *Inpp5j* |
| *Plcb2* | *Ptgs1* |
| *Lrmp* | *Pik3cg* |
| *Hck* | *Cd24a* |
| *Rgs13* | *Ethe1* |
| *Fyb* | *Inpp5d* |
| *Ptpn6* | *Krt23* |
| *Snrnp25* | *Gprc5c* |
| *Kctd12* | *Reep5* |
| *Hpgds* | *Tmem176b* |
| *Tuba1a* | *Ildr1* |
| *Pik3r5* | *Rgs2* |
| *Vav1* | *Pla2g4a* |
| *Tspan6* | *Rbm38* |
| *Skap2* | *Gga2* |
| *Pygl* | *Myo1b* |
| *Ly6g6d* | *Ppp3ca* |
| *Alox5* | *Gimap1* |
| *Bmx* | *Krt18* |
| *Ptpn18* | *2210016L21Rik* |

| **Goblet cell** | |
|---|---|
| *Kdelr3* | *Galnt12* |
| *Tnfaip8* | *Agr2* |
| *Dnajc10* | *Txndc5* |
| *Cmtm7* | *Sdf2l1* |
| *Smim14* | *Stard3nl* |
| *Serp1* | *Ccl9* |
| *Klf4* | *Spink4* |
| *Creld2* | *Tff3* |
| *Pdia5* | *Clca1* |
| *Sec61b* | *Atoh1* |
| *Ern2* | *Guca2a* |
| *Xbp1* | |
| *Nans* | |
| *Scin* | |
| *S100a6* | |
| *Ramp1* | |
| *Muc2* | |
| *Ergic1* | |
| *Pdia3* | |
| *Ssr2* | |
| *Tmed9* | |
| *Creb3l1* | |
| *Slc50a1* | |
| *Qsox1* | |
| *Tmed3* | |
| *Tsta3* | |
| *Foxa3* | |

| | |
|---|---|
| *Nebl* | *Tmem9* |
| *Limd2* | *Fam221a* |
| *Pea15a* | *Atp2a3* |

| |
|---|
| *Wars* |
| *Slc12a8* |
| *Ssr4* |

Supplementary Table 4: Selected outputs from Gene Set Enrichment Analysis

| | ES | NES | NOM p-val | FDR q-val |
|---|---|---|---|---|
| **Small intestine: enriched WT>KO** | | | | |
| REACTOME_CYCLIN_A_B1_B2_ASSOCIATED_EVENTS_DURING_G2_M_TRANSITION | 0.67 | 2.11 | 0 | 0.02 |
| REACTOME_INTERLEUKIN_7_SIGNALING | 0.6 | 1.7 | 0.01 | 0.73 |
| REACTOME_REGULATION_OF_MITOTIC_CELL_CYCLE | 0.42 | 1.7 | 0 | 0.62 |
| REACTOME_CYCLIN_A:CDK2_ASSOCIATED_EVENTS_AT_S_PHASE_ENTRY | 0.4 | 1.66 | 0 | 0.53 |
| REACTOME_REGULATION_OF_PTEN_STABILITY_AND_ACTIVITY | 0.41 | 1.6 | 0.01 | 0.49 |
| BIOCARTA_G2_PATHWAY | 0.5 | 1.58 | 0.03 | 0.43 |
| **Small intestine: enriched KO>WT** | | | | |
| REACTOME_PEROXISOMAL_LIPID_METABOLISM | -0.69 | -2.13 | 0 | 0.01 |
| REACTOME_REGULATION_OF_CHOLESTEROL_BIOSYNTHESIS_BY_SREBP_SREBF | -0.51 | -1.93 | 0 | 0.06 |
| REACTOME_CHOLESTEROL_BIOSYNTHESIS | -0.6 | -1.92 | 0 | 0.05 |
| REACTOME_METABOLISM_OF_STEROIDS | -0.4 | -1.67 | 0 | 0.28 |
| KEGG_STEROID_BIOSYNTHESIS | -0.59 | -1.66 | 0.01 | 0.28 |
| REACTOME_FATTY_ACID_METABOLISM | -0.37 | -1.66 | 0 | 0.26 |
| REACTOME_ACTIVATION_OF_GENE_EXPRESSION_BY_SREBF_SREBP | -0.45 | -1.58 | 0.01 | 0.41 |
| REACTOME_INTERLEUKIN_4_AND_INTERLEUKIN_13_SIGNALING | -0.37 | -1.52 | 0.01 | 0.48 |
| **Lung: enriched WT>KO** | | | | |
| GO_MITOTIC_G2_DNA_DAMAGE_CHECKPOINT | 0.56 | 1.68 | 0.01 | 1 |
| GO_MITOTIC_G2_M_TRANSITION_CHECKPOINT | 0.47 | 1.6 | 0.01 | 1 |
| GO_INTERLEUKIN_7_MEDIATED_SIGNALING_PATHWAY | 0.55 | 1.57 | 0.05 | 1 |
| GO_G0_TO_G1_TRANSITION | 0.42 | 1.55 | 0.03 | 1 |
| REACTOME_INTERLEUKIN_7_SIGNALING | 0.52 | 1.55 | 0.06 | 1 |
| **Lung: enriched KO>WT** | | | | |
| HALLMARK_CHOLESTEROL_HOMEOSTASIS | -0.51 | -2.03 | 0 | 0.37 |
| GO_REGULATION_OF_OXIDATIVE_PHOSPHORYLATION | -0.61 | -1.89 | 0 | 0.79 |

| | | | | |
|---|---|---|---|---|
| GO_STEROL_METABOLIC_PROCESS | -0.42 | -1.65 | 0 | 0.61 |
| REACTOME_INTERLEUKIN_4_AND_INTERLEUKIN_13_SIGNALING | -0.38 | -1.63 | 0 | 0.59 |
| GO_TYPE_2_IMMUNE_RESPONSE | -0.48 | -1.59 | 0.02 | 0.72 |